Advances in Engineering and Technology
An International Journal

Application of Lee Model Curve on Fitting of Discharge Current Curve of Plasma Focus Device

Prakash Gautam*
Department of Science and Humanities, Cosmos College of Management and Technology, Tutepani, Lalitpur

Abstract

A dense plasma focus is a table top machine producing a short-lived extremely popular plasma and cause fusion. Lee Model Code is a computer-based visual basic simulation package, which was successfully utilized in the plasma focus devices. The dynamics of plasma focus discharge is quite complicated, so to review and simplify the complication Lee Model couples electrical circuit with the plasma focus dynamics, radiation and therefore the thermodynamics.This enables us to simulate all of the gross focus properties. In this paper the numerical experiments are carried out to compute the current trace as a function of time for plasma focus (PF) device NX2. Results obtained by the numerical experiments are compared with the published laboratory measured data. This current fitting is completed to get the model parameters.

1. Introduction

1.1 Plasma Focus

A dense plasma focus (DPF) is a machine that produces so hot and a short-lived dense plasma by electromagnetic acceleration and compression that it can cause fusion and emit radiation like x-ray, beam, ionic beam, neutron etc. The electromagnetic compression of the plasma is named asa pinch. It was invented in the early 1960s by J. W Mather and also independently by N. V. Filippov in 1954. It works on the principal of the high-intensity plasma gun device producing plasma as plasmoid. Moreover, in simple a compact pulsed source of radiation is understood as plasma focus[1].

The plasma focus is divided into two sections. The first is a pre-pinch (axial) section. The function of this section is primarily to delay the pinch until the capacitor discharge (rising in a damped sinusoidal fashion) approaches its maximum current. This is done by driving a current sheet down an axial (acceleration) section until the capacitor current approaches its peak. Then the current sheet is allowed to undergo transition into a radial compression phase. Thus, the pinch starts and occurs at the top of the current pulse. This is equivalent.

*Corresponding author
Email: prakashgautam@cosmoscollege.edu.np
Received: March 26, 2021; Revised: May 04, 2021; Accepted: June 26, 2021

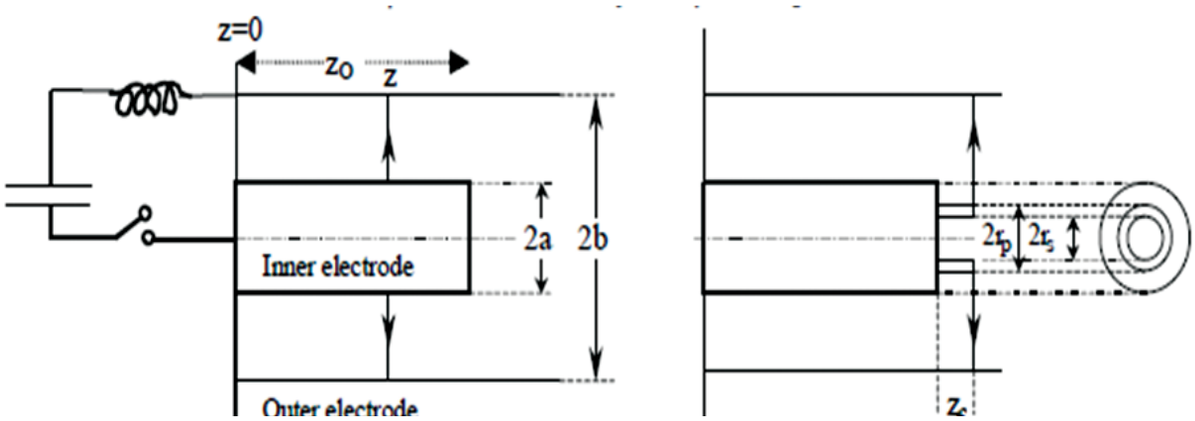

Figure 1: Schematic of the axial and radial phases. The left section depicts the axial phase, the right section the radial phase. In the left section, z is the effective position of the current sheath-shock front structure. In the right section r_s is the position of the inward moving shock front driven by the piston at position r_p. Between r_s and r_p is the radially imploding slug, elongating with a length z_f. The capacitor, static inductance and switch powering the plasma focus is shown for the axial phase schematic only [1].

to driving the pinch with a super-fast rising current; without necessitating the fast line technology. Moreover, the intensity which is achieved is superior to the line driven pinch.

The two-phase mechanism of the plasma focus [1] is shown in figure 1. The inner electrode (anode) is separated from the outer concentric cathode by an insulating backwall. The electrodes are enclosed in a chamber, evacuated and typically filled with gas at about 1/100 of atmospheric pressure. When the capacitor voltage is switched onto the focus tube, breakdown occurs axisymmetrically between the anode and cathode across the backwall. The 'sheet' of current lifts off the backwall as the magnetic field (B_q)and it's inducing current (Jr) rises to a sufficient value [1, 2].

Axial phase: The force pushes the current sheet, accelerating it supersonically down the tube. This is very similar to the mechanism of a linear motor. The speed of the current sheet, the length of the tube and the rise time of the capacitor discharge are matched so that the current sheet reaches the end of the axial section just as the discharge reaches its quarter cycle. This phase typically lasts 1-3 μs for a plasma focuses of several kJ [1, 2, 3].

Radial Phase: The part of the current sheet in sliding contact with the anode then 'slips' off the end 'face' of the anode forming a cylinder of current, which is then pinched inwards. The wall of the imploding plasma cylinder has two boundaries (see figure 1 radial phase). The inner face of the wall, of radius rs is an imploding shock front. The outer side of the wall, of radius rp is the imploding current sheet, or magnetic piston. Between the shock front and the magnetic piston is the annular layer of plasma. Imploding inwards at higher and higher speeds, the shock front coalesces on-axis and a super-dense, super-hot plasma column is pinched onto the axis (see figure 2). This column stays super-hot and super-dense for typically ten ns for a small focus. The column then breaks up and explodes. For a small plasma focus of several kJ, the most intense emission phase lasts for the order of several ns. The radiation source is spot-like (1mm diameter) when viewed end-on [1, 2, 3].

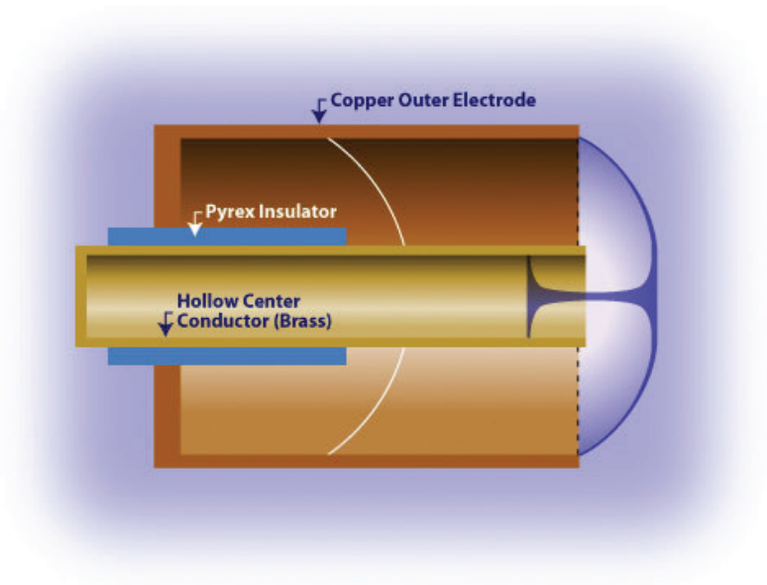

Figure 2: Dense plasma focus device. Image from Glenn Millam. Source: Focus Fusion Society.

Fig.3 shows the shadowgraphs of the plasma focus pinching process. The shadowgraphs are taken at different times. The time period indicates in the shadowgraphs are relative to moment of maximum compression. That moment is taken as t = 0 ns. The standard of the plasma compression is often seen to be excellent, with excellent axisymmetry, and a really well compressed dense plasma.

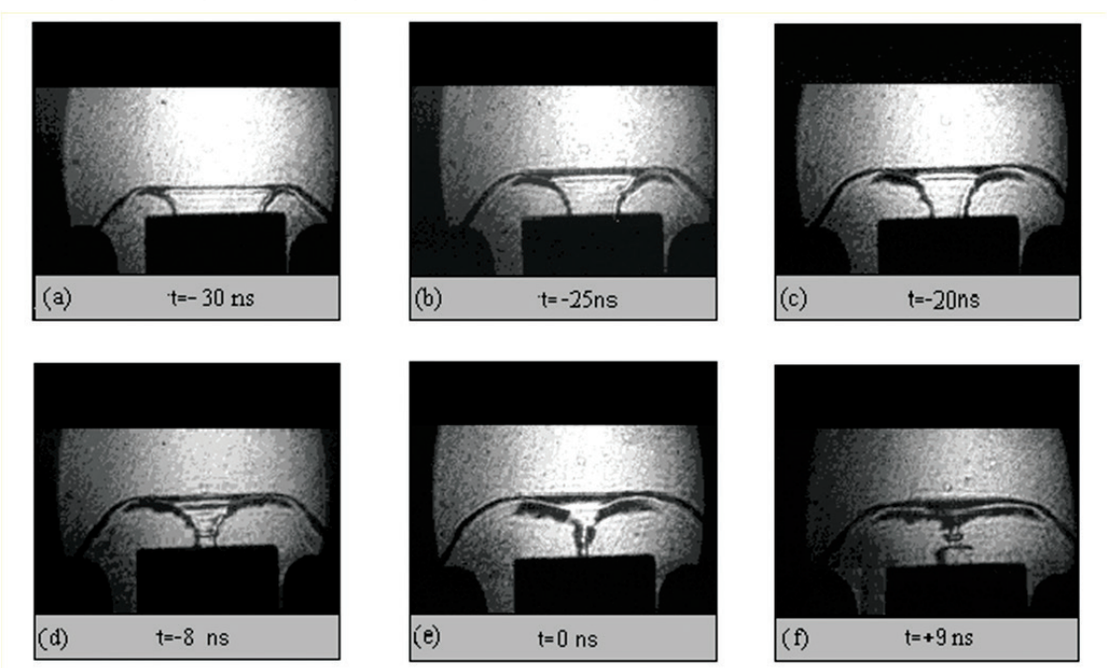

Figure 3: Shadow graphic sequence showing formulation of the plasma focus pinch. Sequential images from(a) to (d) show the plasma column being 'pinched' radially inwards; (e) being time of maximum compression forming the recent and dense 'fusioning' plasma [1].

In the present work, I have done numerical experiments using the Lee Model Code to fit the total discharge current tracefor the DPF machine NX2. NX2 is a second system designed and constructed at Singapore with anode diameter 4 cmand cathode diameter 8 cm made of stainless steel. It is a little table top device with all

components fitting on small table top and is a 3 kJ fourmodel neon operated PF device designed for SXR lithography [4]. Schematic diagram of NX2 PF device is shown in the Fig. 4.

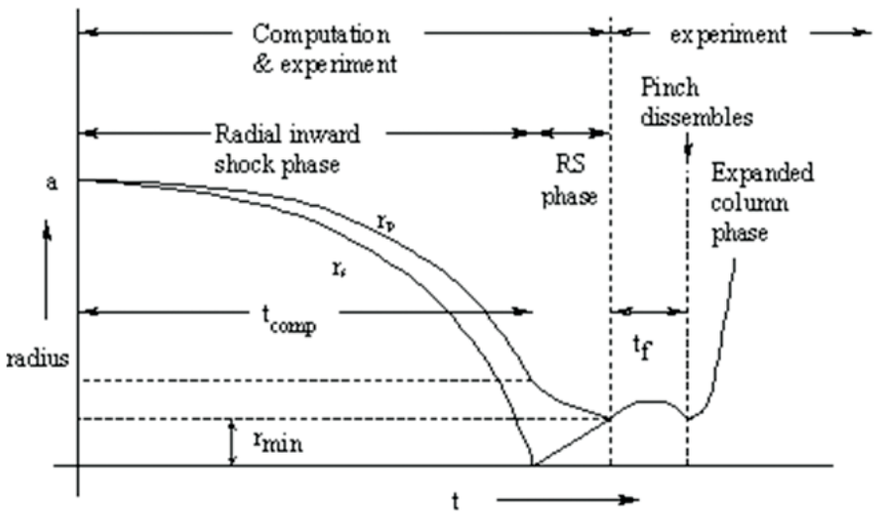

Figure 4: Schematic of radius vs time trajectories to illustrate the radial inward shock phase when r_s moves radially inwards, the reflected shock (RS) phase when the reflected shock moves radially outwards, until it hits the incoming piston r_p leading to the start of the pinch phase (t_f) and finally the expanded column phase [1].

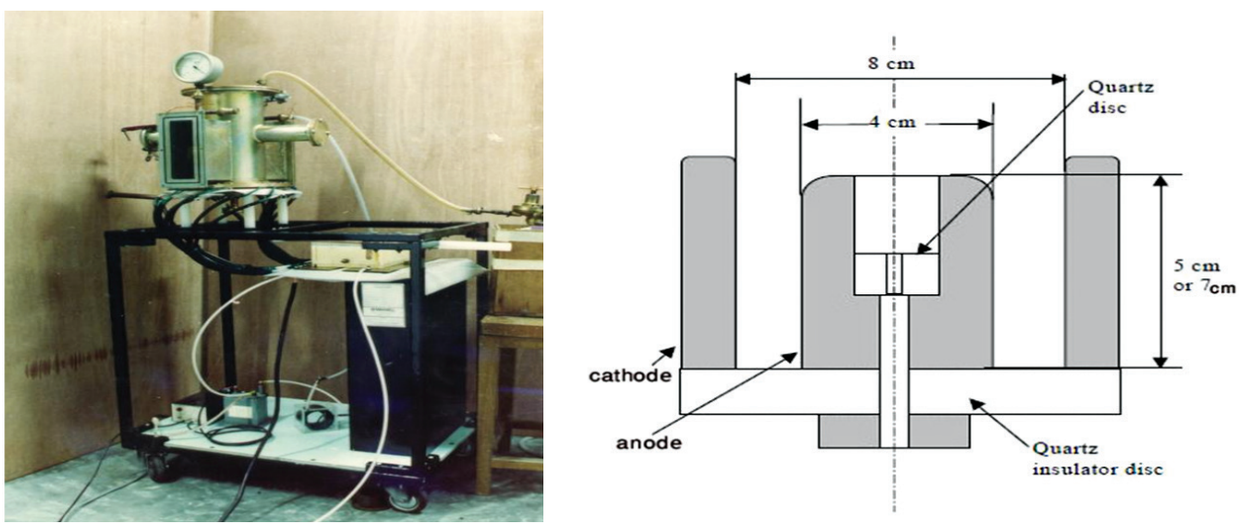

(a) (b)

Figure 5: (a) 3kJ UNU ICTP PFF, b)Schematic diagram of NX2 device [9].

Figure 6: Snapshot of real plasma focus device taken at Plasma research center Guwahati, India.

1.2 The Lee Model Code

Lee organized a network of ten identical DPF machines operates in eight countries round the world in 1986 and is well known by the name Asian African Association for Plasma Training (AAAPT). The Lee Model Code has been developed for this network and is a computer-based simulation package, which was successfully used to assist several experiments the basic model of this is mainly described in 1984 [4, 5]and the newest version of Lee Model Code, which we use here is RADPFV5.15de. The Model Code has been used extensively for all of the Plasma focus including UNU/ICTP PFF, NX2, NX1, and adapted for the Fillippov-type plasma DENA [5]. This Model Code typically creates the superb agreement between experimental data and therefore the computed data. the outline, theory, code and a broad range of results of this 'Universal Plasma Focus Laboratory Facility' are available for download from [4].

Systematically the entire process are divided into five phases. The brief description five phases are summarized as follows [1, 4-6]:

1.3 Axial phase

This phase is described by a snowplow model with an equation of motion coupled to a circuit equation. The equation of the motion includes the axial phase model parameters and easily referred to as mass swept-up and current factors and noted by the symbol fm and fc respectively. fm is liable for porosity of the present sheet, inclination of the movingcurrent sheet shock front structure, physical phenomenon effects and other unspecified effects which creates effects on the quantity of mass within the moving, during the axial phase and fc is liable for fraction of the present effectively driving the structure, during the axial phase. This phase is shown at the left a part of figure 1.

1.4 Radial Inward Shock Phase

This phase described by the four coupled equations using an elongating slug phase. the primary equation calculates the radial inward shock speed from the driving magnetic pressure. The second equation calculates the axial elongation speed of the column. The third one calculates the speed of the present sheath and therefore the fourth equation is that thespeed of the present sheath and therefore the fourth equation is that the speed of the present sheath and the fourth equation is that the circuit equation. because the model parameter fmr and fcr presents as radial mass swept-up and current factor respectively and incorporates for all of the three

radial phases. The model parameter fmr is liable for the consequences which creates effects on the quantity of mass within the moving slug, during the radial phase and fcr is liable for the fraction of the present effectively driving the radial slug. This phase is shown within the right a part of figure 1 and also in figure 4.

1.5 Radial Reflected Shock (RS) Phase

The above four coupled equations also are wont to describe this phase, these being for the reflected shock moving radially outwards, the piston moving radially inwards, the elongation of the annular column and the circuit. An equivalent model parameters fmr and fcr are used as within the previous radial phase. The plasma temperature behind the reflected shocked undergoes a jump by an element on the brink of 2.Numberdensities also are computed using the reflected shock jump equations. This phase is clearly shown in figure 4.

1.6 Slow Compression (Quiescent) or Pinch Phase

Three coupled equations describe this phase: these being the piston radial motion, the pinch column elongation and circuit equation with an equivalent model parameter as within the previous two phases. When the out-going reflected shock hits the in-coming piston the compression enters into the radiative phase. This phase is liable for the emission of the radiation, neutron, ionic beam and electron. The time of transit of the tiny disturbances across the pinched plasma column is about because the duration of the slow compression phase. This phase is additionally shown in figure 4.

1.7 Expanded Column Phase

During this final phase again the Snow Plow model is employed means here again two coupled equations are applied; almost like the axial phase above. This phase isn't taken important because it occur after the main target pinch. it's taken to simulate the present trace beyond the main target pinch point and that we allow the column to suddenly attain the radius of the anode.This phase is additionally seen within the figure 4.

It is noted [7] that in radial phases 2, 3 and 4, axial acceleration and ejection of mass caused by necking curvatures of the pinching current sheath result in time-dependent strongly center-peaked density distributions. Moreover, the transition from phase 4 to phase 5 is observed in laboratory measurements to occur in an extremely short time with plasma/current disruptions resulting in localized regions of high densities and temperatures. These centre-peaking density effects and localized regions are not modeled in the code, which consequently computes only an average uniform density, and an average uniform temperature which are considerably lower than measured peak density and temperature. However, because the four model parameters are obtained by fitting the computed total current waveform to the measured total current waveform, the model incorporates the energy and mass balances equivalent, at least in the gross sense, to all the processes which are not even specifically modeled. Hence the computed gross features such as speeds and trajectories and integrated soft x-ray yields have been extensively tested in numerical experiments for several machines and are found to be comparable with measured values.

2. Methodology

2.1 Fitting of current waveform to modelling for diagnostics

The Lee Model Code was first configured to figure as any of the plasma focus by inputting the tube parameters a, b and z_0 together with the bank parameters L_0, C_0 and therefore the stray resistance r_0 and the operating parameters V_0, P_0 and therefore the gas fill. The tubeparameter of the device shows the dimensions of tube utilized in the plasma focus device, bank parameters showthe capacity of the inductor, capacitance and therefore the resistance utilized in the mixture of circuit of device and operational parameter are operating voltage and therefore the pressure of gas used there.

The quality practice is to fit the computed total current waveform to an experimentally measured total current waveform [3, 6, 8] using four model parameters representing the mass swept-up factor f_m, the plasma current factor fc for the axial phase and factors f_{mr} and f_{cr} for the radial phases.From experience it is recognized that the current trace of the focus is one of the excellent indicators of gross performance. The axial and radial segment dynamics and the indispensable energy transfer into the focus pinch are amongst the important information that is rapidly apparent from the current trace.

The precise time profile of the total current trace is ruled by means of the bank parameters, through the focus tube geometry and the operational parameters. It additionally relies upon on the fraction of mass swept-up and the fraction of sheath current and the variation of these fractions through the axial and radial phases. These parameters determine the axial and radial dynamics, specially the axial and radial speeds which in turn have an effect on the profile and magnitudes of the discharge current. The specific profile of the discharge current in the course of the pinch phase additionally reflects the Joule heating and radiative yields. At the end of the pinch phase the total current profile additionally displays the sudden transition of the current drift from a constricted pinch to a giant column flow. Thus, the discharge current powers all dynamic, electrodynamic, thermodynamic and radiation techniques in the various phases of the plasma focus. Conversely all the dynamic, electrodynamic, thermodynamic and radiation strategies in the various phases of the plasma focus have an effect on the discharge current. It is then no exaggeration to say that the discharge current waveform contains information on all the dynamic, electrodynamic, thermodynamic and radiation processes that takes place in the various phases of the plasma focus. This explains the significance connected to matching the computed current trace to the measured current trace in the technique adopted by using the Lee Model code.

First, the axial model factors f_m, f_c are adjusted (fitted) and then we proceed to adjust (fit) the radial phase model factors f_{mr} and f_{cr}. Note that the fitting of the computed trace with the measured current trace is done up to the end of the radial phase which is typically at the bottom of the current dip. Fitting of the computed and measured current traces beyond this point is not done. If there is significant divergence of the computed with the measured trace beyond the end of the radial phase, this divergence is not considered important.

We configure the code as NX2 using the following extracted parameters (Table I).

Table 1: The Extracted Experimental Parameters For NX2

Bank parameters	Inductance (L_0) = 11.5 nH	From Table no. 5.2 of [9]
	Capacitance (C_0) = 28.8μF	
	Resistance (r_0) = not given	
Tube parameters	Anode diameter (a) = 1.9 cm	From Table no. 6.11 of [9] and Table no. 2 of [9]
	Cathode diameter (b) = 4 cm	
	Anode length (z_0) = 5 cm	
Operating parameters	Charging voltage (V_0) = 11.5 kV	From Table no. 6.12 and Fig. 6.40 (b), 6.42 (a, b, c), 6.43 (b) of [9].
	Gas pressure (P_0) = (1- 5) Torr	

Here, I have been started with trial parameters f_m = 0.06, fc = 0.7, f_{mr} = 0.08 and f_{cr} = 0.7 for NX2.Throughout the fitting process the values of f_c and f_{cr}were kept at 0.7 [1-6], only fine-tuning around this value of 0.7 whenever necessary.

The first step is to fit the axial phase. This involves the variations of the mass swept-up factor (f_m) and the current factor (f_c). As these are varied, the computed total current trace in respect to the rising shape, rise time and Ipeak; and the corresponding measured total current (I_{total}) trace is graphically represented in Fig. 7.

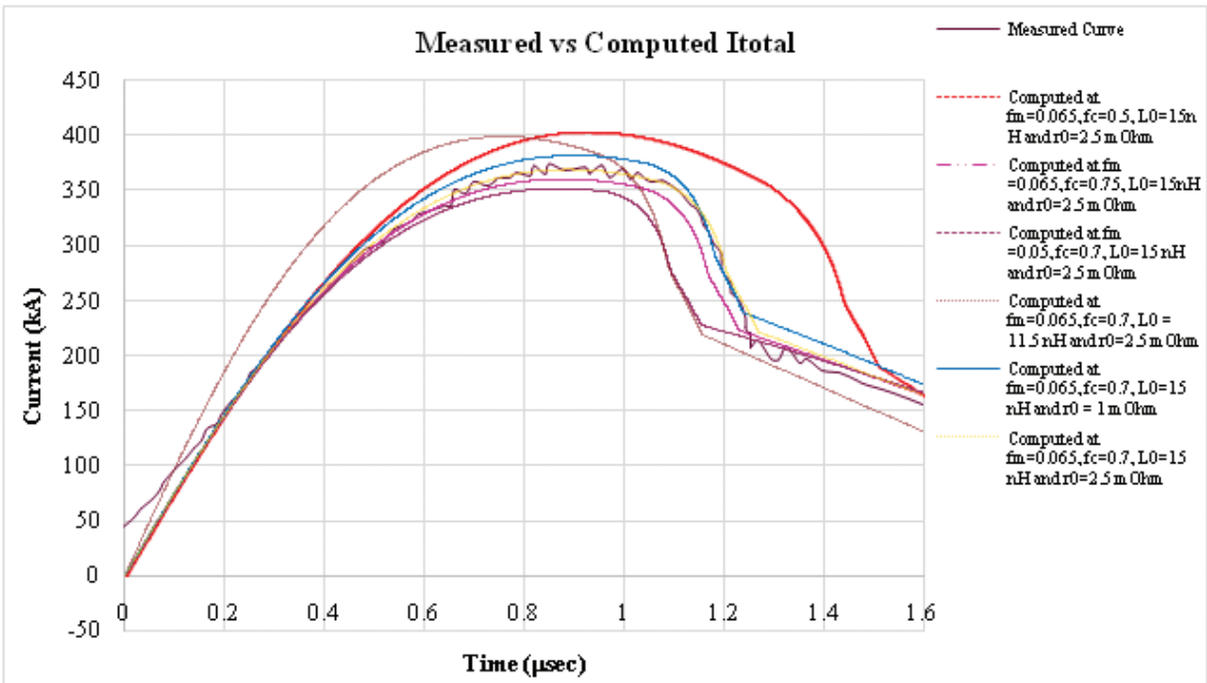

Figure 7: Current fitting of computed current to measured current traces [9] varying axial model parameters including an external static inductance and stray resistance (L_0, r_0) for NX2 with anode length 5 cm operated at 11.5 kV with neon gas at pressure 3 Torr [5].

During the fitting; the increase in fc increases the axial speed; as a result, dynamic resistance increases, hence lowering the current magnitude of the rising slope. These effects are clearly seen in Fig. 7, changing the value of f_c from 0.5 to 0.7. The value of f_c accounts for the fraction of current effectively flowing in the moving structure (due to all effects such as current shedding at or near the back-wall and current sheet inclination). This defines the fraction of current effectively driving the structure, during the axial phase; whereas an increase in fm has an almost inverse effect and also visible from Fig. 7 with changing the values of f_m to the fitted value.

3. Results and Discussions

During the fitting process, the model parameters were varied in steps starting with f_m and f_c, so that the rising slope leading to the topping profile and peak current and the time of focus can be correctly fitted to the measured profile [5, 9].

With the values of f_m and f_c, the value of stray resistance (r_0) needs to be adjusted. I have started with 0.1 × $(L_0/C_0)^{1/2}$ and made the needed adjustment as suggested in r_0 [5]. It has been noted that the decrease in r_0 increases the current trace at all points proportionately. The stray resistance was adjusted to 2.5 mΩ for NX2. Furthermore, in some cases the inductance needs to be adjusted, the inductance L_0 may be given as the short circuit bank inductance. The computed current rise slope is different significantly from the measured slope, so it needs to be adjusted. In adjusting L_0I have noted that increasing L_0 lowers the slope of the rising current, moving from L_0 = 11.5 to 15 nH.

Finally, reasonably good fit is obtainedfor thefollowing bank, tube and operating parameters with slight adjustments to b;

Bank parameters L_0 = 15 nH, C_0 = 28μF r_0 = 2.5 mΩ, tube parameters (cm) b = 4.1 a = 1.9 z_0 = 5 andoperating parameters V_0 = 11.5 kV P_0 = 3 torrNeon. Together with themodel parametersf_m = 0.1, f_c = 0.7, f_{mr} = 0.14 and f_{cr} = 0.69.

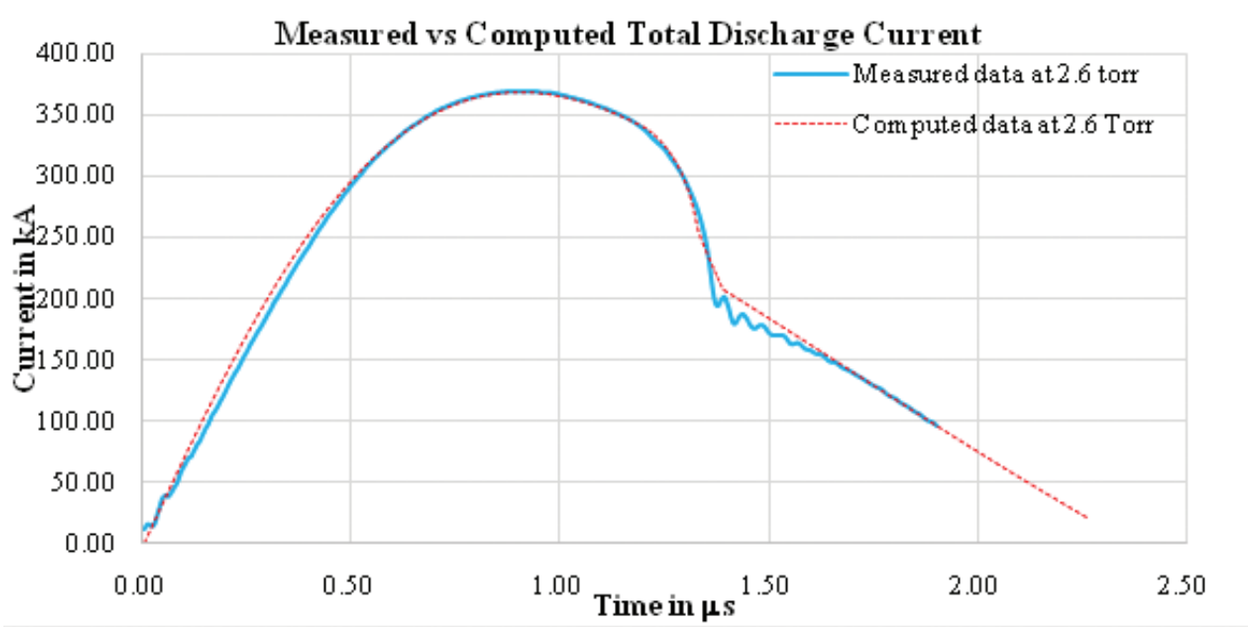

Figure 8: Computed discharge current fitted to the published measured current for NX2 from Fig. 7 (b) of [9] at operating voltage 11.5 kV and pressure 3 torr and anode length of 5 cm. The fitting was done only up to the computed end of the radial phase.

4. Conclusion

The Lee Model Code has been used to fit the numerically measured total discharge current curve with experimental. It was found that the computed current curve fitted well with the published experimental total discharge current trace of the Singaporean plasma focus device NX2. Here advance setting was required to set the inductance and the capacitance either these were wrong or nominal (actual is different from the fitting parameters) and the stray resistance was found to be 2.5 mΩ. Despite these difficulties to fit the computed results were agreed reasonably well with the published curve.

Conflict of Interest

Not declared by the authors.

References

1. Lee S Radiative Dense Plasma Focus Computation Package: RADPF http://www.intimal.edu.my/school/fas/UFLF/File1RADPF.htmhttp://www.plasmafocus.net/IPFS/modelpackage/File1RADPF.htm

2. P. Gautam, R. Khanal, S. H. Saw and S. Lee; Comparison of Measured Soft X-Ray Yield versus Pressure

for NX1 and NX2 Plasma Focus Devices against Computed Values Using Lee Model Code; *J. Fusion Energ.* ***34****, 686–693 (2015).*

3. P. Gautam, R. Khanal, S. H. Saw and S. Lee; Model parameters versus Gas Pressure in Two Different Plasma Focus Devices NX1 and NX2 Operated in Neon; *Trans. Plasma Sci., vol.* ***45,*** *2292-2297, (2017).*

4. S.H. Saw, P. Lee, R.S. Rawat, R. Verma, D. Subedi, R. Khanal, P. Gautam, R. Shrestha, A. Singh and S. Lee; Comparison of Measured Neutron Yield versus Pressure Curves for FMPF-3, NX2 and NX3 Plasma Focus Machines against Computed Results Using the Lee Model Code; *J. Fusion Energ;* ***34****, 474–479 (2015).*

5. S. Lee *et al.*, High rep rate high performance plasma focus as a powerful radiation source, *IEEE Trans. Plasma Sci.*, **26**, no. 4, pp. 1119–1126, (1998).

6. Z. Guixin, Plasma soft X-ray source for microelectronic lithography, Ph.D. dissertation, Nanyang Technol. Univ., Singapore, (1999). [Online available: http://hdl.handle.net/10497/1596]

7. S. Lee S, P. Lee, S H. Saw and R.S. Rawat, Numerical experiments on plasma focus pinch current limitation, *Plasma Phys. Control. Fusion*, ***50***, no. 6, 065 012, (2008).

8. S. Lee, *ICTP Open Access Archive*, (2005). [Online available:http://eprints.ictp.it/85/]

9. Lee S., Saw S. H., Lee P. & Rawat R. S., Numerical Experiments on Neon plasma focus soft x-rays scaling, *Plasma Physics and Controlled Fusion*, ***51***, 105013, (2009).